ISSN 1392–1320 MATERIALS SCIENCE (MEDŽIAGOTYRA). Vol. 22, No. 3. 2016

Fatigue Properties of Welded Butt Joint and Base Metal of MB8 Magnesium Alloy

Ying-xia YU, Bo-lin HE *, Min-hua JIANG, Zong-min LV, Hua MAN

Key Laboratory of Ministry of Education for Conveyance and Equipment, East China Jiaotong University, Nanchang 330013, China

crossref http://dx.doi.org/10.5755/j01.ms.22.3.9132

Received 08 January 2015; accepted 11 September 2015

The fatigue properties of welded butt joint and base metal of MB8 magnesium alloy were investigated. The comparative fatigue tests were carried out using EHF-EM200K2-070-1A fatigue testing machine for both welded butt joint and base metal specimens with the same size and shape. The fatigue fractures were observed and analyzed by a scanning electron microscope of 6360 LA type. The experimental results show that the fatigue performance of the welded butt joint of MB8 magnesium alloy is sharply decreased. The conditional fatigue limit (1×10^7) of base metal and welded butt joint is about 69.41 and 32.76 MPa, respectively. The conditional fatigue limit (1×10^7) of the welded butt joint is 47.2 % of that of base metal. The main reasons are that the welding can lead to stress concentration in the weld toe area, tensile welding residual stress in the welded joint, as well as grain coarsening in the welding seam. The cleavage steps or quasi-cleavage patterns present on the fatigue fracture surface, indicating the fracture type of the welded butt joint belongs to a brittle fracture.
Keywords: MB8 magnesium alloy, welded butt joint, fatigue property, fatigue fracture.

1. INTRODUCTION

As the lightest structural materials with high specific strength and stiffness, magnesium (Mg) alloys have attracted more and more attentions due to the light weight challenge in the automobile and aircraft industry [1 – 4]. Moreover, Mg alloys have also received attention because of their excellent machinability and recyclability. Consequently, it is attractive and promising to achieve high performance and energy saving of machines and structures at the same time by using Mg alloys. From the perspective of crystalline structure, Mg and its alloys always possess a hexagonal close-packed (HCP) structure. As is well known, Mg alloys can be classified into two categories, including the cast alloys and the wrought (rolled, extruded and forged) ones. Compared with the wrought alloys, the cast ones usually have advantages such as cost saving and flexibility in fabrication, while the wrought ones can be extensively applied to load-bearing components in engineering fields where the fatigue failure is the most important failure mode. In view of this, the fatigue properties of wrought Mg alloys should be evaluated carefully [5]. In order to increase the application of Mg alloys in the structure and components of automobile and aircraft industry, the welding process, which can optimize product design and minimize the costs of production, has to be used [6]. Recently, various processes, such as gas tungsten arc welding (GTAW), laser beam welding (LBW), laser-GTAW hybrid welding and friction stir welding (FSW), have been used to investigate the weldability of Mg alloys. Unfortunately, most available literatures pay attention to the effects of welding processes on tensile properties and microstructure of magnesium alloys [7 – 9], but ignore fatigue fracture in metal structures, which causes 80 % to 90 % of failure accidents of welded joints [10]. Experimentally, the influence of friction stir welding on the fatigue behavior of AZ91 alloy was studied by Cavaliere [11]; cyclic deformation and low-cycle fatigue properties of extruded ZK60 alloy were studied by Yu [12]; high cycle fatigue properties of AZ31 alloy were also researched by Somekawa [13], Morita [14], and Ishisara [15]. However, there is little literature available on MB8 magnesium alloy and the influence of welding on fatigue behavior of the welded butt joints of MB8 alloy. Hence, some investigation was conducted in this paper to understand the influence of welding on fatigue properties of welded joints of MB8 magnesium alloy.

2. EXPERIMENTAL DETAILS

2.1. Materials

A commercial MB8 rolled plate with a thickness of 8 mm was used in this study. Table 1 shows the chemical composition of MB8 alloy. The mechanical properties such as yield strength, tensile strength and percentage of elongation of MB8 magnesium alloy and welded joints were evaluated to identify the reasons for variation in fatigue performance. In each condition, three specimens were tested and the average of three results is presented in Table 2.

Table 1. Chemical composition of MB8 (wt.%)

Mn	Ce	Al	Zn	Mg
1.9	0.22	0.25	0.30	Bal.

Table 2. Mechanical properties of welded joint and MB8 base metal

Materials	$\sigma_{0.2}$/MP	σ_b/MPa	δ/%	ν	E/GPa
Base metal	146	239	11	0.33	43
Welded joint	135	201	8	0.33	43
where E – the Young's modulus, $\sigma_{0.2}$ – yield stress limit, σ_b – tensile stress limit, δ is elongation and ν is Poisson' ratio.					

* Corresponding author. Tel.: 0086-0791-87046116; fax: 0086-0791-87046116. E-mail address: *hebolin@163.com* (B. He)

2.2. Welding process

Manual gas tungsten arc welding process was used to weld the MB8 with an MB3 alloy welding wire 3.0 mm in diameter, by virtue of a 300 GP AC/DC TIG welding machine. The welding parameters of the process are presented in Table 3. Before welding, a diameter of 0.2 mm steel wire brush was used to remove oxide film on the groove surface of the MB8 parent metal, and the surface of the specimen was washed with acetone and ethanol.

Table 3. Welding process parameters

Groove type	Welding current, A	Welding voltage, V	Welding speed, $mm \cdot s^{-1}$
x	140 – 160	20 – 24	2.5

2.3. Specimen processing

The MB8 base metal was processed using a wire-cutting machine of DK7732M type (Suzhou, China). The welded joints were first welded and then processed using the same wire-cutting machine. Fig. 1 and Fig. 2 show the shape and size of the fatigue test samples.

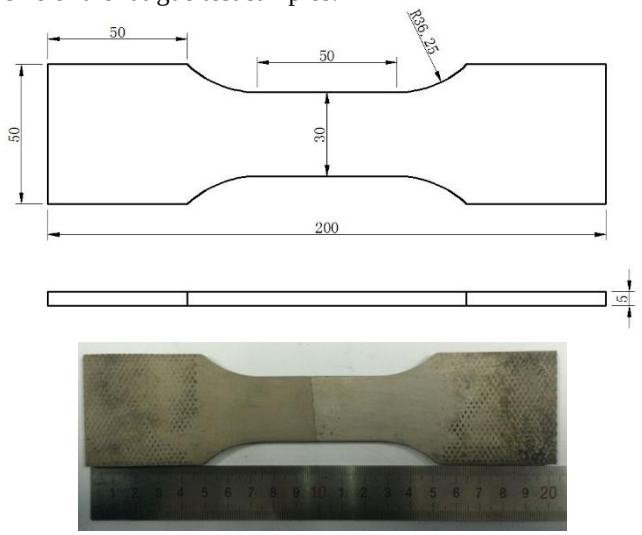

Fig. 1. Shape and size of fatigue samples of MB8 base metal

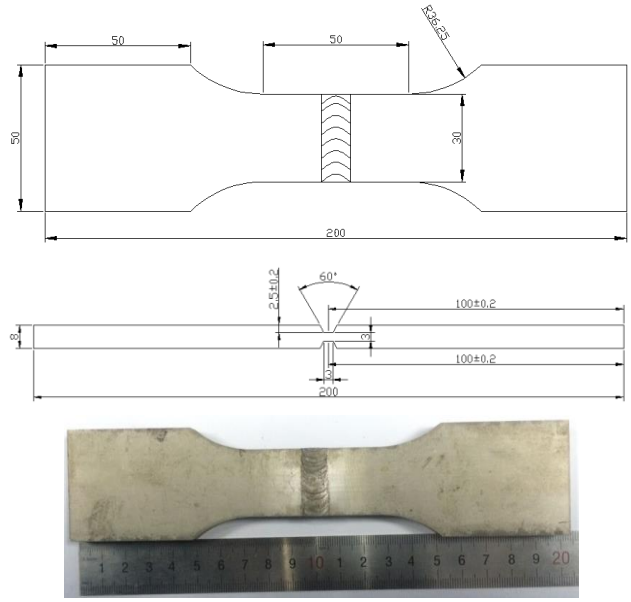

Fig. 2. Shape and size of fatigue samples of MB8 welded butt joint

2.4. Fatigue test procedures

Load controlled tension-tension fatigue tests were performed on EHF-EM200K2-070-1A type fatigue testing machine (RICOH, Japan) with the ratio of minimum load versus maximum as r = 0.1. The frequency used for testing all the specimens was set as 10Hz.

2.5. Microstructure and fracture surface observation

The microstructures of the cross section of MB8 base metal and welded butt joint were observed using the BX41M-LED type optical microscope (Zeiss, Germany). The fatigue fracture surfaces of MB8 base metal and the weld butt joint were observed by means of SJM-6360LA type scanning electron microscopy (JEOL, Japan). The samples for microstructure observation were cut from the MB8 base metal and welded butt joint, and then ground and mechanically polished. Afterwards, the samples were immerged into a 4 % nitric acid alcohol solution to obtain the microstructure.

3. RESULTS AND DISCUSSION

3.1. Microstructure and analysis

The microstructures of MB8 base metal and the welded butt joint under optical microscopy are shown in Fig. 3.

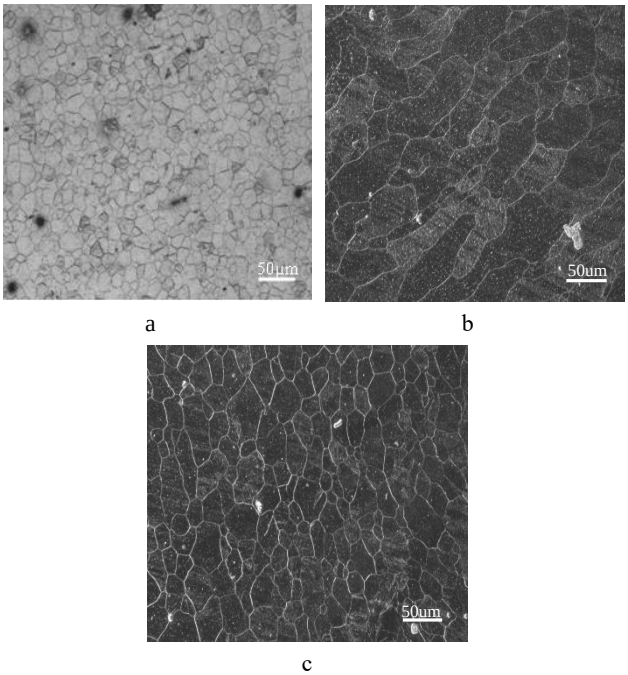

Fig. 3. Microstructures of MB8 alloys: a – base metal; b – weld seam; c – heat affected zone

From the micrographs, it can be seen that the average grain size in the weld region, heat affected zone and base metal was approximately 70 μm, 40 μm and 20 μm, respectively. It is obvious that the grains in the butt weld region (Fig. 3 b) and heat affected zone (Fig. 3 c) were larger than those of base metal (Fig. 3 a), and that the grains in the weld region were the largest. That is to say, grain coarsening in the weld zone occurs after welding process, and it will be unfavorable to the fatigue life of welded joints [16].

3.2. Fatigue test results and analysis

Fatigue tests were conducted using EHF-EM200K2-070-1A type electro hydraulic fatigue testing machine with a stress ratio of 0.1 and a testing frequency of 10 Hz. The fatigue properties of MB8 samples and the welded butt joint were tested, and the results are presented in Table 4 and Table 5, respectively.

Table 4. Fatigue test results of MB8 base metal

Specimen	Stress range, $\Delta\sigma_{max}$/ MPa	Cycle number to failure, N/10^6	Failure zone
1	90	0.042	Transition zone
2	90	0.054404	Transition zone
3	85	0.136409	Transition zone
4	82.5	0.123387	Transition zone
5	80	0.543504	Transition zone
6	77.5	1.053376	Transition zone
7	75	5.794976	Transition zone
8	70	10.15632	Unfaulted

Table 5. Fatigue test results of welded butt joint

Specimen	Stress range, $\Delta\sigma_{max}$/ MPa	Cycle number to failure, N/10^6	Failure zone
1	47.5	0.156572	Weld toe
2	45	0.254596	Weld toe
3	42.5	0.376138	Weld toe
4	40	0.666954	Weld toe
5	37.5	1.275797	Weld toe
6	35	7.176906	Weld toe
7	32.5	10.346654	Unfaulted

For the MB8 base metal, the samples 1 to 7 were all failed in the transition zone while the sample 8 is un-fractured until 1×10^7 cycles, as shown in Table 4. In contrast, the samples 1 to 6 for the welded butt joint were all failed in the weld toe, while the sample 7 was un-fractured until 1×10^7 cycles (see Table 5).

By means of the fatigue test values in Table 4 and Table 5, S-N curves of the MB8 base metal and welded butt joint could be plotted, as shown in Fig. 4.

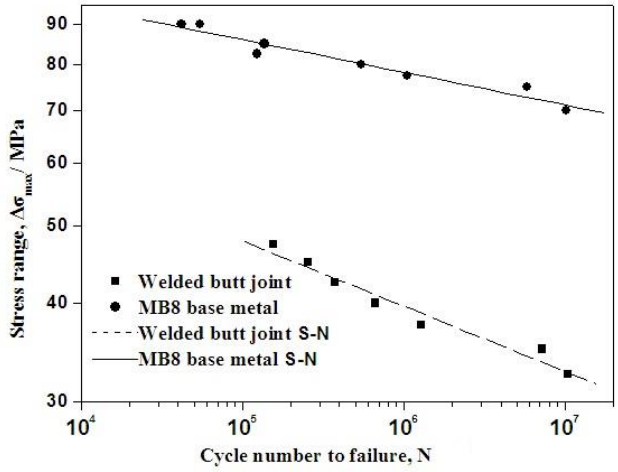

Fig. 4. S-N curves of MB8 and welded butt joints

The fatigue test data were divided into two parts by the S-N curves, of which the bottom were the fatigue test results of the welded butt joint, and the upper were those of the base metal of MB8.

Table 6 indicates that corresponding to a 70 % survival rate, the fatigue strength of the MB8 base metal and welded butt joint is 69.41 MPa and 32.76 MPa, respectively. That is to say, the fatigue strength of the joint is 47.2 % of that of base metal. This indicates that there is a 52.8 % reduction in fatigue strength values due to welding. The main reasons can be attributed to the stress concentration in the weld toe, the tensile welding residual stress in the weld joint, and the grain coarsening in the weld and heat affected zones. The stress concentration coefficient of the specimen is quite different for base metal and welded joint, and the fatigue load carrying capacity has very close relationship to the stress concentration coefficient of the specimen. The parameters in Table 6 can properly fit formula $N(\Delta\sigma)^m = Cm$, here, m and Cm are material constants.

Table 6. Parameters of S-N curve of MB8 base metal and welded joint

Specimen	m	Cm	$\Delta\sigma$, MPa
Base metal	22.7	48.8	69.41
Welded joint	15.38	30.3	32.76

The fatigue crack initiation site, propagation direction and fracture position of MB8 base metal and the welded butt joints is shown in Fig. 5.

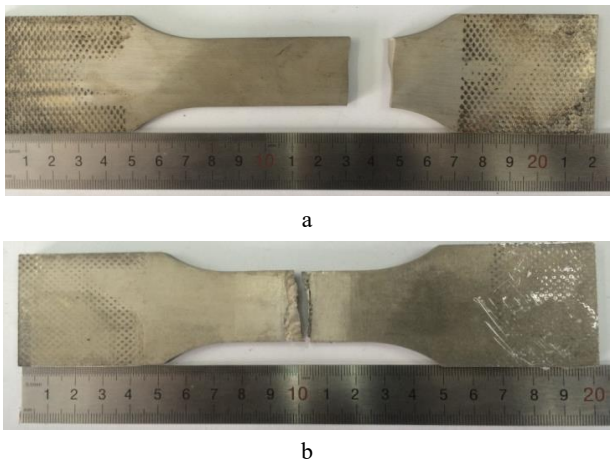

a

b

Fig. 5. Fatigue crack initiation site, propagation direction and fracture site: a – the base metal; b – the welded joint

Fig. 5 a represents that the fatigue crack in the base metal specimen initiates at the transition zone between gauge length and clamp part, and then propagates along the direction that is vertical to the load direction. As shown in Fig. 5 b, it can also be noticed that the position of welding toe is the crack initiation site for the welded joint, and the crack propagation direction is along the fusion line due to the coarse microstructure. Fig. 6 shows the calculation result of stress distributions of welded butt joint using the ABAQUS finite element program.

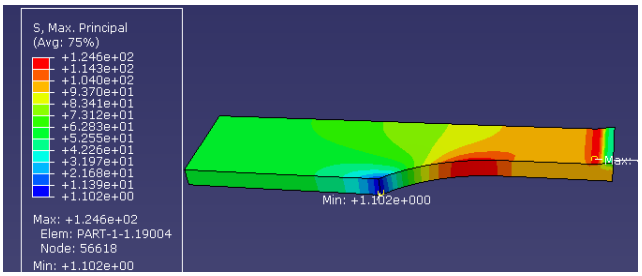

Fig. 6. Max principal stress distribution of specimen

Because the stress concentration is more significant in the positions of welding toe and transition zone as shown in Fig. 6, the crack normally initiates at these sites.

3.3. Fatigue fracture analysis

Fig. 7 shows the fatigue fracture surfaces of MB8 base metal and the welded butt joint.

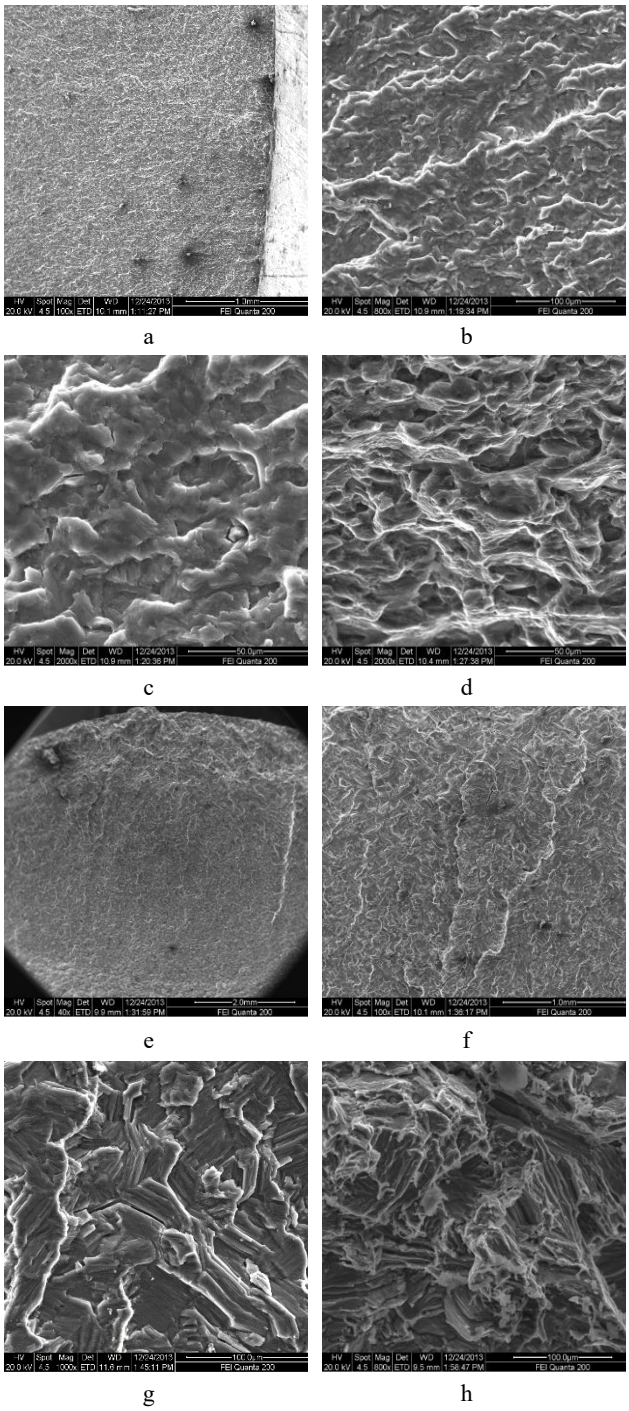

Fig. 7. SEM images of fatigue fracture surfaces: a – crack initiation site; b – crack propagation zone; c – secondary cracks in base metal; d – torn edges on the fracture surface; e – crack initiation site of welded joint; f – fracture surface of butt joint; g – secondary cracks in butt joint; h – the final fracture zone of butt joint

Fig. 7 a, b, c and d show the fracture surfaces of MB8 base metal. As Fig. 7 a and b illustrate, the fatigue crack initiates at the specimen surface, and the fracture surface presents quasi-cleavage and fan-shaped patterns in the propagation zone of fatigue crack. On the fracture surface, some secondary cracks can be observed, and Fig. 7 c shows the partially enlarged image of Fig. 7 b (indicated with a black arrow). Fig. 7 d indicates the last fracture zone. Tear ridges can be found on the quasi-cleavage fracture surface (indicated with a black arrow). Besides, some dimples can be observed on the fracture surface, which are typical morphologies of a ductile fracture. Fig. 7 e, f, g and h show the fracture surfaces of the welded joint. Fig. 7 e illustrates that the fatigue crack also initiates at the specimen surface. Fig. 7 f shows a secondary crack on the fracture surface (indicated with black arrows), and some cleavage steps can be observed on the fatigue fracture surface of the joint, as Fig. 7 g shows, and there are also secondary cracks on the fracture surface. In Fig. 7 h, many cleavage steps can be found, which exhibits a brittle fracture for the welded butt joint.

Relative to the ideal hard sphere value of pure Mg (1.732) [17], Mg and its alloys have an HCP structure with a smaller c/a (c is lattice height, a is the side length of the base plane) ratio of 1.624. It is well known that the plasticity deformation capacity of Mg alloys mainly depends on the c/a ratio. Compared to FCC and BCC metals with twelve slip systems, the plasticity deformation capacity of Mg alloys, which has only 3 slip systems, is weak. Its plasticity deformation relies not only on slip, but also on twinning. It presents a brittle fracture characteristic while failed. The crack shape is strongly changed due to the plastic deformation occurring on the high index plane. A quasi-cleavage fracture character appeared on the fatigue fracture surface with a few secondary cracks. Due to the non-uniform grain size, some crack forks may form during crack propagation, and these forks will inhibit crack propagation to some extent. This inhibition effect can result in the higher fatigue strength for the MB8 base metal. However, in the weld toe, there may be inevitable tensile welding residual stresses, coarse grains and stress concentration, thus leading to a lower fatigue strength of the welded joint.

4. CONCLUSIONS

1. The conditional fatigue limit (1×10^7) of MB8 base metal and welded butt joint is about 69.41 and 32.76 MPa, respectively. The conditional fatigue limit (1×10^7) of the welded butt joint is 47.2 % of that of the base metal. The main reason can be attributed to the stress concentration in the welded toe zone, the tensile welding residual stress in the weld joint, as well as the grain coarsening in the weld and the heat affected zone.
2. For MB8 Mg alloy base metal, the crack initiates at the specimen surface. For butt joint, the crack also initiates at the weld toe surface and propagates along the fusion line. The crack propagation presents a transgranular pattern.
3. There are a lot of secondary cracks in the crack propagation zone, and cleavage steps or quasi-cleavage patterns can be observed on the fatigue fracture surface, indicating a brittle fracture occurs.

Acknowledgements

The authors would like to thank the financial support from the National Natural Science Foundation (No. 51265013), the Natural Science Foundation of Jiangxi Province (No. 20114BAB206020) and the Science Foundation of education office of Jiangxi Province (GJJ12302).

REFERENCES

1. **Agnew, S.R., Mehrotra, P., Lillo, T.M., Stoica, G.M., Liaw, P.K.** Texture Evolution of Five Wrought Magnesium Alloys During Route an Equal Channel Angular Extrusion: Experiments and Simulations *Acta Materialia* 53 (11) 2005: pp. 3135 – 3146.
2. **Morita, S., Ohno, N., Tamai, F., Kawakami, Y.** Fatigue Properties of Rolled AZ31B Magnesium Alloy Plate *Transactions of Nonferrous Metals Society of China* 20 2010: pp. s523 – s526.
   http://dx.doi.org/10.1016/S1003-6326(10)60531-6
3. **Keiro, T., Masaki, N., Yoshihiko, U.** Fatigue Crack Propagation and Fracture Mechanisms of Wrought Magnesium Alloys in Different Environments *International Journal of Fatigue* 31 (7) 2009: pp. 1137 – 1143.
4. **Chen, Z.H., Yan, H.G., Chen, J.H., Quan, Y.J., Wang, H.M., Chen, D.** Magnesium Alloy, Chemical Industry Press, Beijing, 2004. (in Chinese)
5. **Yoshihiko, U., Toshifumi, K., Masaki, N., Yuki, N., Satoshi, M., Hiroshi, M.** Fatigue Crack Propagation of AZ61 Magnesium Alloy Under Controlled Humidity and Visualization of Hydrogen Diffusion Along the Crack Wake *International Journal of Fatigue* 59 (2) 2014: pp. 234 – 243.
6. **Padmanaban, G., Balasubramanian, V., Madhusudhan Reddyb, G.** Fatigue Crack Growth Behaviour of Pulsed Current Gas Tungsten Arc, Friction Stir and Laser Beam Welded AZ31B Magnesium Alloy Joints *Journal of Materials Processing Technology* 211 (9) 2011: pp. 1224 – 1233.
   http://dx.doi.org/10.1016/j.jmatprotec.2011.02.003
7. **Afrin, N., Chen, D.L., Cao, X., Jahazi, M.** Microstructure and Tensile Properties of Friction Stir Welded AZ31B Magnesium Alloy *Materials Science and Engineering A* 472 (1 – 2) 2008: pp. 179 – 186.
8. **Quan, Y.J., Chen, Z.H., Gong, X.S., Yu, Z.H.** Effects of Heat Input on Microstructure And Tensile Properties of Laser Welded Magnesium Alloy AZ31 *Materials Characterization* 59 (10) 2008: pp. 1491 – 1497.
   http://dx.doi.org/10.1016/j.matchar.2008.01.010
9. **Padmanaban, G., Balasubramanian, V., Sarin Sundar, J.K.** Influences of Welding Processes on Microstructure, Hardness and Tensile Properties of AZ31B Magnesium Alloy *Journal of Materials Engineering and Performance* 19 (2) 2010: pp. 155 – 165.
   http://dx.doi.org/10.1007/s11665-009-9389-7
10. **Zhang, H.X., Wang, W.X., Wei, Y.H., Li, J.Y., Wang, J.L.** Fatigue Fracture Mechanism of AZ31B Magnesium Alloy and Its Welded Joint *Transactions of Nonferrous Metals Society of China* 21 (11) 2011: pp. 1225 – 1233.
11. **Cavaliere, P., De Marco, P.P.** Fatigue Behaviour of Friction Stir Processed AZ91 Magnesium Alloy Produced By High Pressure Die Casting *Materials Characterization* 58 (3) 2007: pp. 226 – 232.
    http://dx.doi.org/10.1016/j.matchar.2006.04.025
12. **Yu, Q., Zhang, J.X., Jiang, Y.Y., Li, Q.Z.** An Experimental Study on Cyclic Deformation and Fatigue of Extruded ZK60 Magnesium Alloy *International Journal of Fatigue* 36 (1) 2012: pp. 47 – 58.
    http://dx.doi.org/10.1016/j.ijfatigue.2011.08.016
13. **Somekawa, H., Maruyama, N., Hiromoto, S., Yamamoto, A., Mukai, T.** Fatigue Behaviors and Microstructures in Extruded Mg-Al-Zn Alloy, *Materials Transaction* 49 (3) 2008: pp. 681 – 684.
    http://dx.doi.org/10.2320/matertrans.MRP2007292
14. **Morita, S., Tanaka, S., Ohno, N., Kawami, Y., Enjoji, T.** Cyclic Deformation and Fatigue Crack Behavior of Extruded AZ31B Magnesium Alloy *Materials Science Forum* 638 – 642 2010: pp. 3056 – 3061.
15. **Ishisara, S., Nan, Z., Goshima, T.** Effect of Microstructure on Fatigue Behavior of AZ31 Magnesium Alloy *Materials Science and Engineering A* 468 – 470 2007: pp. 214 – 222.
16. **Zhen, R., Fang, X.X., Sun, Y.S., Yang, X.** Progress in Research on Fatigue Behavior of Wrought Magnesium Alloys *Materials Review* 24 (9) 2010: pp. 130 – 133. (in Chinese)
17. **Yu, Q., Zhang, J.X., Jiang, Y.Y., Li, Q.Z.** An Experimental Study on Cyclic Deformation and Fatigue of Extruded ZK60 Magnesium Alloy *International Journal of Fatigue* 36 (1) 2012: pp. 47 – 58.
    http://dx.doi.org/10.1016/j.ijfatigue.2011.08.016